NOTICE

CERTAIN DATA CONTAINED IN THIS DOCUMENT MAY BE DIFFICULT TO READ IN MICROFICHE PRODUCTS.

Conf-9005145--5

CONF-9005145--5

DE91 006088

[001] TILT GRAIN BOUNDARIES IN $YBa_2Cu_3O_{7-x}$ THIN FILMS*

Y. Gao,[1] G. Bai,[2] H.L.M. Chang,[2] K.L. Merkle[2] and D.J. Lam[2]

[1]Science and Technology Center for Superconductivity and
[2]Materials Science Division
Argonne National Laboratory
Argonne, IL 60439

JULY 1990

DISCLAIMER

*This work was supported by the National Science Foundation (DMR88-09854) through the Science and Technology Center for Superconductivity (YG) and by the U.S. Department of Energy, Offices of Basic Energy Sciences-Materials Science (GB, HLMC, KLM, DJL) under contract No. W-31-109-Eng.-38.

Manuscript submitted to the ***Frontiers of Electron Microscopy in Materials Science Conference,*** Oak Brook, IL, May 20-24, 1990.

[001] TILT GRAIN BOUNDARIES IN $YBa_2Cu_3O_{7-x}$ THIN FILMS

Y. Gao, G. Bai, H. L. M. Chang, K. L. Merkle and D. J. Lam

Materials Science Division, Argonne National Laboratory

Argonne, IL 60439

ABSTRACT

Grain boundaries in $YBa_2Cu_3O_{7-x}$ superconductor thin films grown on (001) MgO by metal-organic chemical vapor deposition (MOCVD) have been characterized using transmission electron microscopy (TEM) and high-resolution electron microscopy (HREM). It was found that the $YBa_2Cu_3O_{7-x}$ thin films were highly textured with the c axes, or [001] orientation, nearly parallel between grains and perpendicular to the MgO substrate. A majority of the grain boundaries are low-angle boundaries with a tilt angle, θ, less than 15°. The low-angle boundaries appear to be strongly faceted on an atomic scale in such a way that the boundary planes tend to be parallel to the (100), (010), or (110) lattice planes in one of the adjacent grains. Almost all of the lattice planes, except for a number of distorted regions along the boundaries, are continuous across the boundaries from one grain to another, accommodating the misorientation with a slight bending of the lattice planes. The small-angle boundaries are shown to consist of arrays of dislocations. A domain structure, formed by the interchange of a and b axes has been observed in large grains. The domain boundaries are strongly faceted with the (100) and (010) lattice planes parallel to the boundaries. These observations on the atomic structure of boundaries, are used to discuss the effect of grain boundaries on superconductor properties in $YBa_2Cu_3O_{7-x}$ thin films.

INTRODUCTION

The importance of grain boundaries on the superconductivity of $YBa_2Cu_3O_{7-x}$ can be seen by comparing the critical current density of polycrystalline samples [1] ($10 \sim 10^3$ A/cm^2 at 77 K) with that of single crystals [2,3] ($> 10^5$ A/cm^2 at 77 K). By measuring the superconducting properties of individual grain boundaries, Chaudhari et al. [4] have presented direct evidence that the critical current density across a grain boundary is always significantly less than that of either adjacent grain. The amount of the reduction varied for different grain boundaries, which indicates that this important superconducting property depends on the grain boundary structure or grain boundary misorientation. Subsequently, Dimos et al. [5] demonstrated a strong correlation between the critical current densities across the grain boundaries and the grain boundary misorientations. It was found that the ratio of the critical current density across the grain boundaries (J_c^{gb}) to the average value of the critical current densities in the adjacent grains (J_c^{G}) decreases dramatically over the misorientation range from 0 to 15°. After 15°, this ratio reaches a saturation value, almost 2 orders of magnitude smaller than that for θ=0. This relationship indicates that high critical current densities could be obtained in polycrystalline materials if the materials are highly oriented with small misorientations between grains. It has been demonstrated by a number of investigators that highly-textured bulk samples with the c axes aligned between grains yield 2 to 3 orders of magnitude higher critical current densities than those obtained in non-textured bulk materials. Moreover, the critical current densities in c axis-oriented thin films can be obtained as high as in single crystalline thin films. Consequently, the acquisition of a detailed picture of the atomic structure, composition and defect morphology of grain boundaries, together with an understanding of their influence on the grain boundaries' electric properties, has become a central issue in the investigation of these materials. A number of possible causes for the weak links in these materials have been proposed based on their defect structure. However, most of the extrinsic defects, such as second phase

layers at grain boundaries, amorphous material at grain boundaries, and micro-cracks, can be avoided by better material processing. Therefore, in well-prepared polycrystalline materials the intrinsic character of the grain boundaries must be responsible for the poor intergrain coupling. On the other hand, grain boundaries in highly-oriented thin films and highly textured polycrystals can also have a positive effect on the supercurrent by providing structures suitable for flux pinning.

It is well known that low-angle tilt boundaries consist of a wall of edge dislocations, each with Burgers vector **b** and spaced $|\mathbf{b}|/\theta$ apart, where θ is the tilt angle. Low-angle twist boundaries are comprised of a network of screw dislocations. In general, a low-angle grain boundary contains an array of mixed dislocations with both edge and screw components. In all cases, the misfit associated with the misorientation is concentrated at the dislocation cores.

At large misorientations, the description of a grain boundary in terms of dislocations is inappropriate, since the core regions would be overlapping and be extremely closely spaced. It is important to recognize that grain boundaries could possibly assume a great multitude of structures, since a general boundary already requires for its macroscopic description five geometric parameters. For tilt GBs four degrees of freedom are however sufficient to describe their macroscopic geometry.

Among the possible arrangements of grains relative to each other a strong selection, or preference for certain arrangements is expected, particularly in anisotropic structures, such as the high-temperature superconducting cuprates. The population of GBs that is present in a given material depends on which GBs are preferred, i.e. are low in energy, as well as on kinetic factors, which can often be controlled by processing conditions.

The atomic-scale structure of GBs is extremely important for the transport properties of high-T_c oxide superconductors. In contrast to metals, GBs in ceramic oxides,

due to their largely ionic bonding, are expected to have more open structures [6]. This is thought to be due to the fact that ions with like charges ions cannot lie in close proximity. In cubic oxides indications for a reduced atomic density due to the incorporation vacancy-type defects into the GB has been found experimentally [7]. Therefore, the grain boundaries in the $YBa_2Cu_3O_{7-x}$ material may contain large open spaces, either in the form of an open structure, or by the incorporation of point defects. An open structure at [100] low-angle tilt boundaries in $YBa_2Cu_3O_{7-x}$ has been reported [8]. In these boundaries considerable structural disorder seemed to be associated with the dislocation cores. In spite of these observations, an understanding of the grain boundary structure in $YBa_2Cu_3O_{7-x}$ on an atomic scale is still quite rudimentary, at best. Moreover, the atomic structure of highly-oriented MOCVD grown thin films has not been investigated. For example, it is not known, whether the dislocation cores at low-angle grain boundaries differ from one to another. Since the structure of the $YBa_2Cu_3O_{7-x}$ superconductor is much more complex compared to metals and simple ceramics, it is inevitable that the atomic structure of the quite large unit cells in these materials is significantly modified in the immediate vicinity of the GB. Therefore, significant differences of composition and structure may exist at the grain boundary dislocation cores, compared to the bulk. An understanding of these structural and compositional differences will be very important for unravelling the mystery of the effects of planar defects on superconducting properties.

From this perspective, the present work was undertaken to obtain information about the atomic structure of the [001] tilt grain boundaries in highly-oriented $YBa_2Cu_3O_{7-x}$ thin films. The thin films were grown on (001) MgO by metal-organic chemical vapor deposition (MOCVD) and had the c axes closely parallel between different grains and perpendicular to the substrate surface . The observations are used to discuss the role of the defects on superconducting properties in the MOCVD thin films.

EXPERIMENTAL

The $YBa_2Cu_3O_{7-x}$ thin films were grown by the MOCVD method in a low pressure, cold wall, horizontal system. The 2,2,6,6-tetramethyl-3,5-heptanedionates of Y, Ba, and Cu were used as starting materials. The organometallic precursor vapors of these compounds were mixed and introduced into the reactor by high-purity nitrogen as carrier gas. The flow rates of the carrier gas and the oven temperatures for each of the precursor chambers were individually controlled. The oven temperature was centered at 130 °C, 230 °C, and 120 °C for Y, Ba, and Cu, respectively. Slight variations (within ± 20 °C) of these temperature settings were used to optimize deposition conditions. The thermal decomposition of the vapor mixture was carried out on a heated substrate in a low pressure (5-15 Torr) quartz reactor. Pure oxygen was used as an oxidant and was introduced into the reactor in a separate line.

Three kinds of substrates were used, namely, (001) $SrTiO_3$, (001) MgO and (001) YSZ. Substrate temperatures ranging from 700 to 900 °C were employed in the present study. After deposition, the thin films were cooled in oxygen at a pressure of one atmosphere. The cooling rate was 10 °C/min down to 200 °C, whereupon the films were brought to room temperature by turning off the heater. In most cases, all three types of the substrates were placed simultaneously on a susceptor to study the effect of the substrate on the film morphology and microstructure. A detailed description has been reported elsewhere [9]. The thin films used in the present study were grown on (001) MgO. In general, the $YBa_2Cu_3O_{7-x}$ thin films grown on (001) MgO are highly-oriented polycrystalline films with the c axes parallel between grains and perpendicular to the substrate surface. The superconducting transition temperature of the films in the as-grown condition was determined by magnetization measurements to be approximately 84 K using a low field (0-50 Oe) SQUID magnetometer.

TEM planar samples were prepared by mechanical thinning, dimpling, and argon ion milling from the MgO side using a liquid nitrogen cooled stage. . The high-resolution electron microscopy (HREM) of grain boundary structures was performed using a H-9000 operating at 300 kV, at the Dept. of Materials Science, Northwestern University. Chemical microanalysis and material characterizations were carried out by using a Philips 420 equipped with an x-ray energy dispersive spectrometer (XEDS) and an electron energy loss spectrometer (EELS).

RESULTS

Two different film morphologies were obtained within the range of growth conditions used. Transmission electron microscopy (TEM) shows that both thin films are highly-oriented polycrystals with the c axes parallel between grains (< 2°), and that the orientations of the grains in the a-b plane appear rather random throughout the films. Most of the [001] tilt angles between the grains are less than 15°, which indicates that the majority of the grain boundaries are low-angle grain boundaries. The XEDS analysis shows that the films consist largely of the $YBa_2Cu_3O_{7-x}$ superconductor with a limited number of isolated second phases. However, the first film has a large grain size (~ 3 μm), and the grain boundaries are micro-faceted. On the other hand, the second film has a much smaller grain size (~ 0.5 μm), and the grain boundaries are rather straight.

A representative TEM image of the first film is shown in Fig. 1a. The twin structures in the film can be clearly seen, indicating that the as-grown film was orthorhombic after cooling to room temperature. Fig. 1a shows a grain boundary as indicated by a number of arrows. The tilt angle was determined from the selected-area electron diffraction pattern to be about 21° . Note that the grain boundary is strongly faceted; therefore it is quite difficult to recognize the grain boundary in fig.1a. Within each

grain, a number of small particles (marked by the letter P in fig. 1a) can be observed. Some of them are $YBa_2Cu_3O_{7-x}$ grains with a different orientation, while others consist of secondary phases. One should also note, that a high density of dislocations exists in both grains. The selected-area electron diffraction pattern in Fig. 1b, taken from grain A, shows a small arc at each diffracted spot, which indicates that a number of low-angle grain boundaries are present ($\theta<4°$) inside grain A. In other words, some of the observed dislocations may be primary grain boundary dislocations belonging to low-angle grain boundaries. However, it is very difficult to confirm this by conventional TEM. Therefore, these grain boundaries were investigated by high-resolution electron microscopy (HREM). The HREM studies demonstrate that some of the dislocations are indeed edge dislocation walls of low-angle grain boundaries.

Fig. 2 shows a HREM image of a low-angle grain boundary with $\theta=3.5°$. The white spots in the image represent the metal columns. Two sets of lattice fringes, namely the (100) and (010) fringes, are visible in both grains. By close inspection of the image, one can find three dislocations along the grain boundary (central part of the image), as indicated by arrows. The (010) lattice planes are symmetric about the dislocation cores. By drawing a Burgers circuit around a dislocation, it can be shown that the Burgers vector, **b**, of the dislocations is equal to a[100] . These dislocations have a spacing (D) of 6 nm, which is consistent with the value calculated from Franks formula, $D=|\mathbf{b}|/\theta$. It is noted that the dislocation cores are localized within a few lattice parameters. The surrounding matrix shows only a slight lattice distortion, and the (100) fringes, or the (100) lattice planes, are slightly bent, but continuous across the grain boundary. By careful examination of the dislocation cores, it is found that the structure image at the dislocation cores is different from that in the adjacent grains, which indicates that the material at the dislocation cores may not be superconducting. A detailed study of the dislocation core structure by computer simulation is underway. Such defects, if not superconducting, may be strong pinning

centers. Since the film contains a very high density of such defects, the pinning force could be very strong in this type of film.

At some grain boundaries, the dislocation cores appear delocalized. In most cases, the delocalization of the dislocation cores is associated with micro-faceting and steps at the grain boundaries. This kind of delocalization often causes strong lattice distortions at the grain boundaries. Fig. 3 shows an example of such a delocalization, associated with micro-faceting. A low-angle grain boundary with θ=4° can be seen in the low-magnification TEM image (Fig. 3a). The grain boundary consists of a set of defects which show some strain contrast. The HREM image in Fig. 3b gives a clear picture that the grain boundary is strongly faceted, and the strain contrast is associated with the lattice distortion at grain boundary dislocations. The dislocation cores are delocalized at the distorted regions. A Burgers circuit around one distorted region was successfully drawn, and a closure failure was found to be one (100) interplanar spacing (Note that no distinction between the (100) and (010) planes was made in this case). The average spacing of the distorted regions is about 8.5 nm, which is not in agreement with the calculated value, about 5.5 nm. One may note that in Fig. 3b, two sets of the lattice fringes, namely (100) and (010) fringes, are visible in grain 1, while only (220) fringes are visible in most areas of grain 2. This is due to a slight thickness difference between the two grains as can be seen in Fig. 3a. Therefore, this sample is not suitable to study the detailed structure of the delocalized dislocations. However, by a careful inspection of the image, it can be found that the grain boundary, which is inclined by ~ 30° to one set of the fringes in grain 1, is faceted to be parallel to the (100), (010), and (110) lattice planes so that one set of the (220) fringes are continuous across the grain boundary. The delocalization of the dislocation cores is also associated with micro-steps at grain boundaries. An example is given in Fig. 4 for a low-angle grain boundary with θ=1°. The HREM image shows that the grain boundary is almost parallel to the (010) lattice planes in the adjacent grains, and that a

number of the steps with a height of one (100) interplanar spacing are formed at the boundary as indicated by arrows. A large distorted region in the top grain appears associated with one of the steps. By making a large Burgers circuit around the region, one finds a closure failure equal to the (100) lattice spacing. It is interesting to note that in addition to delocalized dislocation cores, localized dislocations were found at the same boundary which are associated with only a slight amount of lattice distortions. An example of such a dislocations is shown by the letter L in Fig. 4. Such dislocations are similar to the ones in Fig. 2.

Micro-faceting at low-angle grain boundaries was commonly observed in MOCVD thin films. In all cases, the grain boundaries have a tendency to facet in such a way that the faceted boundaries will be parallel to the (100), (010), or (110) lattice planes in one of the adjacent grains. However, the faceting at some grain boundaries is associated with strong lattice distortions, while the faceting at others causes only slight distortions. It was found, in general, that the distortion was correlated with the inclined angle between the grain boundary plane and one of the three low-index lattice planes. If the inclined angle is large, the distortion will be strong. This correlation has been demonstrated by a number of observations. Fig. 5 gives an example where a small segment of the low-angle grain boundary (θ=7.5°), as indicated by the letter A, is almost parallel to the (110) planes in one grain, while another segment, indicated by the letter B, deviates from (110) by a small inclination. It can be seen in Fig. 5a that only small strain contrasts are associated with segment A. However, quite strong strain contrast is observed at segment B. The HREM image of the segment A in Fig. 5b shows that there is no further faceting at the segment. When the image is viewed under a shallow angle perpendicular to the boundary, the continuity of one set of the (220) lattice fringes across the boundary and the slight bending of lattice planes can be easily recognized. A number of dislocations with small lattice distortions can be observed at the segment, as indicated by arrows. The Burgers vector of

these dislocations was determined to be {(a+b)/2}[110]. However, the atomic structure of the dislocation cores can not be determined from this image. An enlarged view of segment B, Fig. 5c, shows that the grain boundary is faceted in a such way that the faceted boundary is parallel to the (110), and (010) lattice planes. Strong strain contrast associated with the faceting indicates that the lattice distortions are connected with faceting. By a careful inspection of the image, one can note that one set of the (220) lattice fringes is discontinuous across the boundary in the central part of the image. By drawing a Burgers circuit around this region, it was found that there exists a dislocation with Burgers vector equal to {(a+b)/2}[110]. However, the dislocation core is somewhat delocalized.

Fig. 6 shows another example of low-angle grain boundary faceting. A low-magnification image of the grain boundary (θ=3°) in Fig. 6a shows two strongly inclined macroscopic-scale facets. The angle between segment A and B is about 40°, indicating that the two segments are bounded by different lattice planes. A HREM image of the segment A in Fig. 6b shows that the segment is bounded by one set of the (110) planes. Micro-faceting in this segment with the (010) plane parallel the boundary can also be observed (see arrows). A dislocation with Burgers vector {(a+b)/2}[110] is found for this segment. The (010) lattice planes, except at the dislocation cores, are continuous across the boundary in this section. A different kind of faceting was found at segment B, see Fig. 6c, where the grain boundary is almost parallel to the (010) lattice planes. It can easily be seen, viewing the micrograph under a shallow angle, that most of the (100) lattice fringes continue across the boundary. Burgers vectors equal to a[100] or b[010] can also be determined at some of the distorted regions by drawing a Burgers circuit. However, the dislocation core structure can not be obtained, since the dislocation cores are delocalized. Nevertheless, the grain boundary appears very dense without any indication for large open spaces.

At some grain boundaries, complex dislocation configurations were observed. The dislocations could dissociate into two dislocations with a smaller Burgers vector. An example is given in Fig. 7a, which shows a grain boundary with θ=4.5°. Strong, extended strain contrasts can be seen along the boundary. The contrast, in some regions, appears in pairs at both sides of the boundary, while at others it appears only at one side of the boundary. The spacing between the strained regions ranges from 2 nm to 5 nm. A HREM image of the segment with a pair of the strained regions, as shown in Fig. 7b, indicates that the shape of the strained regions are determined by the character of the dislocations The Burgers vector of the dislocations was found to be a[100] in one grain, and b[010] in other grain. However, the dislocation cores of both kinds appear delocalized. If a large Burgers circuit covering a pair of the dislocations is drawn, one can find that the closure failure is equal to (a+b)[110]. Therefore, one may suggest that the observed dislocations should be considered dissociated dislocations. In other words, the dislocations with Burgers vector (a+b)[110] are dissociated into two dislocations with the smaller Burgers vectors a[100] and b[010]. This argument is supported by the observation of the Burgers vector (a+b)[110] at the segment with the one-side strained regions. As is well known, the elastic energy of a dislocation is proportional to $|\mathbf{b}|^2$, where **b** is the Burgers vector. Thus, the total energy can be reduced by the dissociation into dislocations with a smaller Burgers vector.

So far, only the low-angle grain boundaries have been presented and discussed. In order to study the difference of the atomic structure between the low-angle and the high-angle boundaries, HREM of a few high-angle boundaries has been carried out. Fig. 8 shows a HREM image of a high-angle grain boundary. Actually, the image shows three grains converging at a triple point. The angle between grain 1 and 2, or between grain 1 and 3, is about 41°, while the angle between grain 2 and 3 is less than 1°. A dislocation with a Burgers vector {(a+b)/2}[110] can be observed at the 2/3 boundary, as indicated by

an arrow. Comparing grain 1 and 2, it is found that the (100) lattice fringes (Note that no distinction between the (100) and (010) lattice fringes was made here.) in grain 1 are almost parallel to one set of the (110) fringes in grain 2. About 70% of the (110) fringes in grain 2 appear to be continuous across the boundary with a highly localized distortion at the grain boundary, and connect with the (100) fringes in grain 1. That is, about 30% of the (110) lattice fringes in grain 2 terminate at the boundary. One may also note that the structure of the grain boundary appears almost as dense as the low-angle boundaries. Since the density of the terminated lattice fringes is so high, it becomes impossible to determine the Burgers vector of the dislocations at the boundary. The short segment near the triple point in Fig. 8 has (310) and (210) planes in grain 1 and 2 respectively, nearly parallel to each other. Therefore, this asymmetric GB is formed from relatively low-index planes. A similar structure is found at the 1/3 boundary near the triple point. However, this boundary is faceted in such a way that the faceted boundary is closely parallel to the (110) and (100) lattice planes in grain 1. A second facet, involving the same planes as in grain 1/2 is formed near the bottom of the image.

Domain structures, or the grain boundaries with θ=90°, are also commonly observed in the films. The domains were typically found inside of large grains. An example is shown in Fig. 9a, where the domain walls are strongly faceted, and are parallel to the (100) and (010) planes. An enlarged image of segment A in Fig. 9b indicates that the domain walls are coherent boundaries. No dislocations have been observed at the domain walls.

DISCUSSION

It is known that two aspects are important in the correlation between the structural defects of a superconductor and its performance regarding critical currents: flux pinning and weak links. Concerning the first aspect, the material must contain sufficient pinning

centers to prevent flux creep. Since the pinning centers are regions of inhomogeneities in the lattice [10], resulting in local changes in Tc, structural variations must be incorporated in the structure. The best type of flux-pinning defects are those, whose size in the plane perpendicular to the fluxoids is rather localized and does not extended over a region larger than the period of the flux line lattice [10,11]. If the defect is smaller than the flux line lattice parameter, the pinning force is proportional to the radius of the defect [10,11]. Obviously low-angle grain boundaries can act as strong flux pinning centers for flux line movement since the boundaries consist of a number of localized defects. On the other hand, the grain boundaries can also act as weak links since the coherence length, over which the Cooper pair can tunnel over a non-superconducting region, is very small, about 2 ~ 3 nm perpendicular to the c axis and 0.5 nm parallel to the c axis.

It has been reported that critical current densities (J_c) as high as ~ 10^7 A/cm^2 can be obtained for c axis oriented thin films [12]. Recently, Muto et al. [13] reported that for the best film prepared by MOCVD, the critical current density, ~ $3x10^4$ A/cm^2, was obtained by resistive measurement in a very high magnetic field, 27 T. This indicates that there exist strong flux pinning capacities in such films. With respect to the J_c value of the oriented thin films, the J_c value of polycrystalline materials with random grain boundaries is much smaller, e. g. 10 ~ 10^3 A/cm^2. Since no structural differences occur between the oriented thin films and polycrystalline materials, one must conclude that the grain boundary structure is the main cause for low Jc values in polycrystalline materials. On the other hand, grain boundaries in thin films seem to have a positive effect on Jc.

It has been shown in the present study that lattice fringes at adjacent grains of the low-angle grain boundaries are continuous across the boundaries with a slight bending. The grain boundary structure is almost as dense as that in the grains except for a number of the distorted regions. A small fraction of the lattice fringes terminated at the boundaries are observed, which correspond to the grain boundary dislocations in low-angle grain

boundaries. Discrete grain boundary dislocations could act as a barrier to the flow of supercurrent or as pinning sites since it is known that the structural disorder and the lattice distortion are associated with weak links and flux pinning. The number of the terminated fringes, or the density of the dislocations, depends on the tilt angle. When the tilt angle becomes larger, the dislocation density will increase proportionally. Therefore, more lattice fringes are terminated at the boundary, which indicates that the critical current densities across the grain boundaries will decrease as the tilt angles increase. The reduction in J_c has been observed by Dimos et al [5]. With increasing the tilt angles, the dislocation cores eventually overlap so that the grain boundary is no longer composed of discrete dislocations. Therefore, there is no good area at the grain boundaries so that the superconducting coupling at the boundaries is strongly reduced.

Studies of the grain boundary structure in polycrystalline high-temperature superconductors has shown that a rather open structure is observed at the boundaries [8,14]. In most cases, the lattice fringes are not connected well at the boundaries due to the large misorientation between adjacent grains. Even at some low-angle grain boundaries, the structure still appears open since the grain boundaries in polycrystalline materials are commonly observed to be joined by the (001) planes [8,14]. In contrast, the grain boundary structure appears always rather dense in the c oriented films, no matter whether the misorientation is large or small. This observation can be compared to the results from atomic structure observations on <001> tilt grain boundaries in NiO, where large-angle GBs typically also appear quite dense and well-structured [7,15]. In this case a considerable concentration of vacancy-type defects seem to be associated with large-angle GBs. The incorporation of point defects at the GB may also be an important factor determining the superconducting properties of GBs in $YBa_2Cu_3O_{7-x}$. Very important in this regard is the observed micro-faceting at most of the low-angle grain boundaries in the present films, which results in good connections between grains, and retains discrete

dislocations at grain boundaries. Since the majority of the grain boundaries in the films are low-angle boundaries, the faceting could play an important role concerning the superconducting properties of thin films.

CONCLUSIONS

The highly-oriented $YBa_2Cu_3O_{7-x}$ superconductor thin films with the c axes or [001] orientation, nearly parallel between grains and perpendicular to the substrate surface, have been prepared on (001) MgO by metal-organic chemical vapor deposition (MOCVD). It was found that the majority of the grain boundaries are low-angle boundaries with a tilt angle ,θ, less than 15°. The low-angle boundaries appear to be strongly faceted on an atomic scale in such a way that the boundary planes tend to be parallel to the (100), (010), or (110) lattice planes in one of the adjacent grains. Almost all of the lattice planes, except for a number of distorted regions along the boundaries, are continuous across the boundaries from one grain to another, accommodating the misorientation by a slight bending of the lattice planes. This indicates that the grain boundaries in the thin films are connected very well. The grain boundaries have a much more dense structure compared with the structure in polycrystalline materials. The small-angle boundaries are shown to consist of arrays of dislocations. Some of the dislocation cores are localized, whereas others appear somewhat delocalized. The lattice distortions associated with most of the low-angle grain boundaries are commensurate with the distance between GB dislocations. On the other hand, no long-range strains are observed at high-angle grain boundaries, since lattice distortions associated with GB core structures strongly overlap, leaving the GB disorder strongly localized at the boundary.

A domain structure caused by the interchange between the a axis and the b axis has been observed in large grains. The domain boundaries are strongly faceted with the (100) and (010) lattice planes parallel to the boundaries. The boundaries are coherent without any

dislocations. Such a domain structure might be typical to the film growth process, since no observations of this type of structure has been reported for bulk samples. The effect of the domain structure on the superconducting properties could be the same as for twin structures since both types of boundaries are coherent.

ACKNOWLEDGEMENTS

This work was supported by the National Science Foundation (DMR88-09854) through the Science and Technology Center for Superconductivity (YG) and by the U. S. Department of Energy, Offices of Basic Energy Sciences - Materials Science (GB, HLMC, KLM, DJL) under contract No. W-31-109-ENG-38. The use of the H-9000 in the Dept. of Mater. Sci. & Enger., Northwestern University is gratefully acknowledged.

REFERENCES

[1] J. W. Ekin, Adv. Ceram. Mat. **2**, 586 (1987).

[2] T. R. Dinger, T. K. Warthington, N. J. Gallagher and R. L. Sandstrom, Phys. Rev. Lett., **58**, 2687 (1987).

[3] P. Chaudhari, R. H. Koch, R. B. Laibonitz, T. R. Mcguire and R. J. Gambino, Phys. Rev. Lett., **58**, 2684 (1987).

[4] P. Chaudhari, J. Mannhart, D. Dimos, C. C. Tsuei, J. Chi, M. M. Oprysko and M. Scheurmann, Phys. Rev. Lett., **60**, 1653 (1988).

[5] D. Dimos, P. Chaudhari, J. Mannhart and F. K. Legoues, Phys. Rev. Lett., **61**, 219 (1988).

[6] D. M. Duffy and P. W. Tasker, Phil. Mag. A **47**, 817 (1983).

[7] K. L. Merkle and D. J. Smith, Phys. Rev. Lett. **59**, 2887 (1987).

[8] M. F. Chisholm and D. A. Smith, Phil. Mag. A, **59**, 181 (1989).

[9] G. R. Bai, Y. Gao, H. Shi, H. L. M. Chang, J. C. Parker and D. J. Lam, Submitted to Proceedings of the 7th CIMTEC World Ceramices Congress - Satellite Symposium 4, "High Temperature Superconductors", Trieste, Italy, July 2-5, 1990.

[10] E. J. Kramers, J. Nucl. Mat., **72**, 5 (1978).

[11] G. P. van der Mey, and P. H. Kes, Phys. Rev. B, **29**, 6233 (1988).

[12] T. Terashima, K. Iijima, K. Yamamoto, Y. Bando and H. Mazaki, Jap. J. Appl. Phys., **27**, L91 (1988).

[13] Y. Muto, K. Watanabe, N. Kobayashi, H. Kawabe, H. Yamane, H. Kurosawa, and T. Hirai, Physica C, **162**, 105 (1989).

[14] H. W. Zandbergen and G. van Tendeloo, Mat. Res. Soc. Symp. Proc., **156**, 209 (1989).

[15] K. L. Merkle and D. J. Smith, Ultramicroscopy **22**, 57 (1987).

Figure Captions

Fig. 1 a) A typical plan-view TEM micrograph of the YBCO thin films grown on (001) MgO by MOCVD. A grain boundary with a tilt angle θ=21° is shown by arrows. b) A selected-area diffraction pattern taken from grain A shows a small arc at each diffracted spot, indicating that the grain consists of a number of grains with small relative misorientations.

Fig 2 Three dislocations indicated by arrows are observed at a low-angle grain boundary (θ=3.5°). The dislocations are very localized and their Burgers vector is equal to a[100]. The dislocation core structure appears different from that in the adjacent grains, indicating that the core material may not be superconducting.

Fig. 3 a) Low-magnification image of a low-angle grain boundary (θ=4°) which consists of a number of discrete defects. b) HREM image shows that the boundary is strongly faceted and dislocation cores are delocalized at the distorted regions.

Fig. 4 A large distorted region at a grain boundary (θ=1°) is associated with micro-steps indicated by arrows. The localized dislocations are also observed at the boundary as shown by the letter L.

Fig. 5 a) Low-magnification image of a low-angle grain boundary (θ=7.5°). b) HREM image of segment A in a) shows that the boundary plane is parallel to one set of the (110) lattice planes in the bottom grain. A number of dislocations with Burgers vector {(a+b)/2}[110] are observed at the boundary as indicated by arrows. c) HREM image of segment B shows that the boundary is micro-faceted in such a way that the faceted boundary is parallel to the (110) and (010) lattice planes.

Fig. 6 a) Low-magnification image of a curved boundary with θ=3°. The boundary is faceted so that the boundary plane at segment A is parallel to the (110) lattice planes as shown in b), while segment B is parallel to the (010) lattice planes as shown in c).

Fig. 7 a) Strong strain contrast is observed at a grain boundary (θ=4.5°). The spacing between the strained regions ranges from 2 nm to 5 nm. b) HREM image shows that the strained regions are associated with the dislocation character. At the segment with a pair of the strained regions, the Burgers vector is equal to a[100] in one grain, and b[010] in the other grain. However, the Burgers vector is (a+b)[110] at the segment with the strained regions at one side of the boundary, indicating the former dislocations are dissociated.

Fig. 8 HREM image of high-angle grain boundaries (θ=41°) between grain 1 and 2, or grain 1 and 3, shows that about 30% of the (110) lattice planes in grain 2 and 3 are terminated at the boundaries with a very localized lattice distortion. A discrete dislocation is observed at the low-angle boundary between grain 2 and 3, as shown by an arrow.

Fig. 9 a) Low-magnification HREM image of a domain structure introduced by interchange between a and b axes. b) Enlarged image of segment A in a) shows that the domain walls are coherent.


P
P
P
A
B
0.3 μm

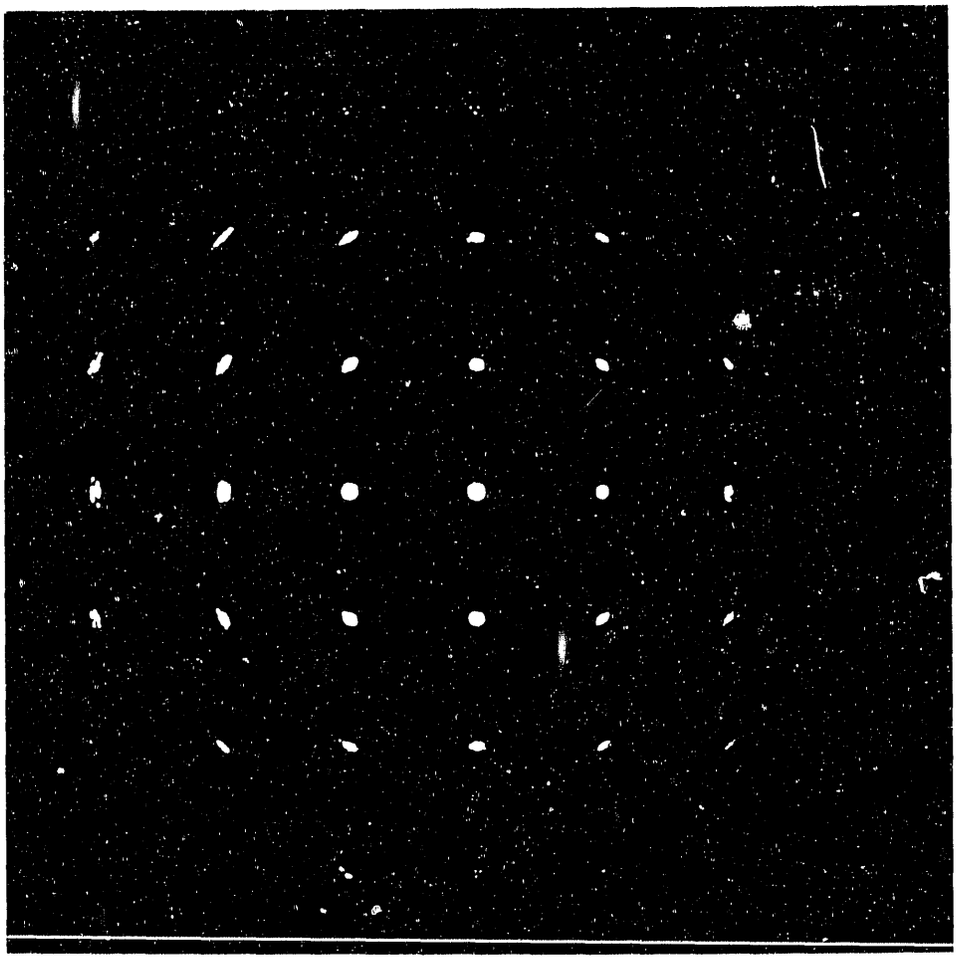

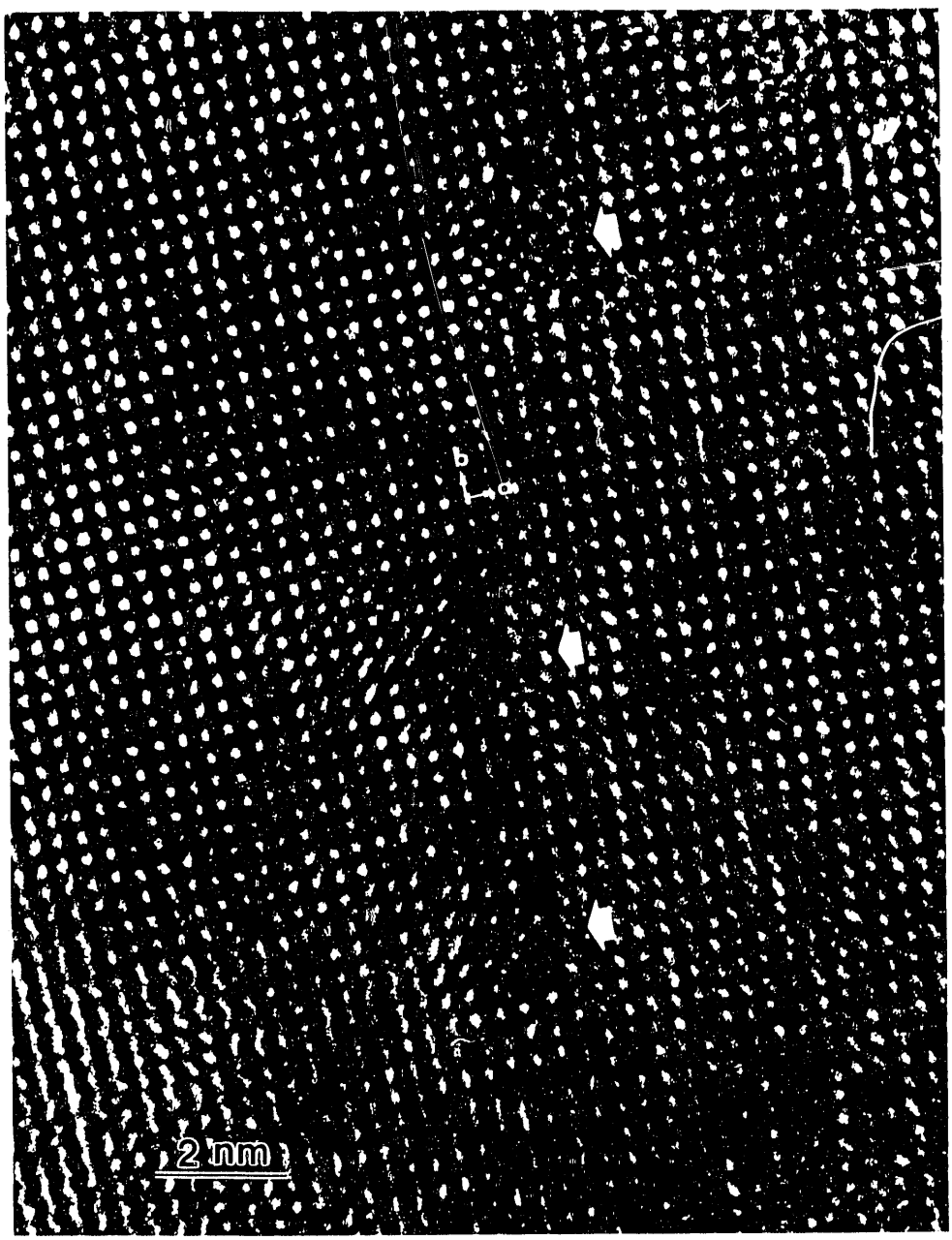

Fig. 2

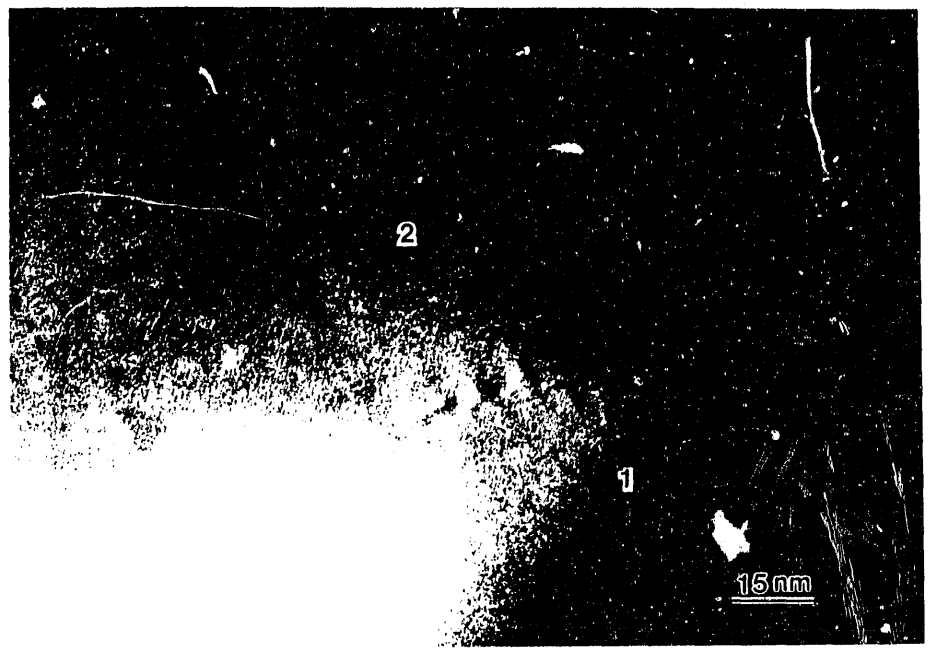

Fig. 3a

2 nm
N

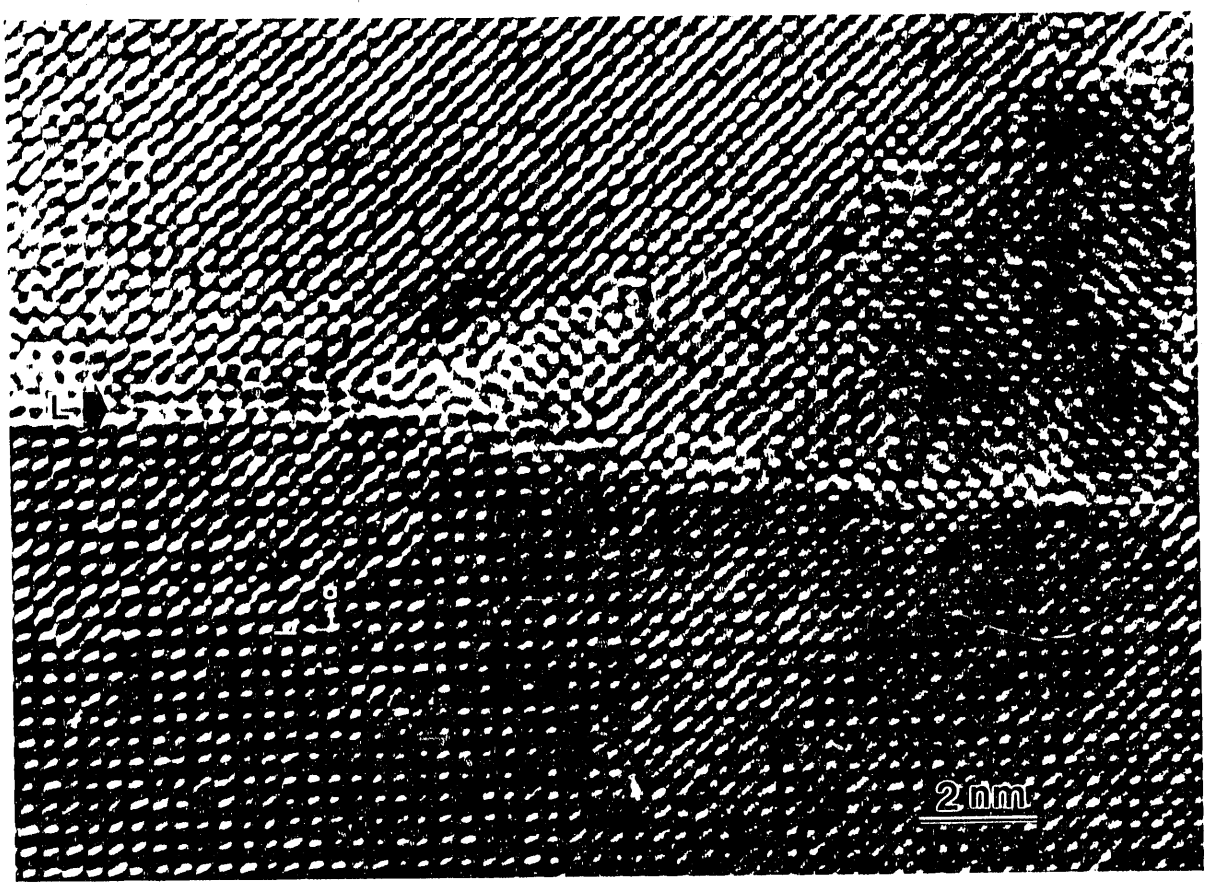

Fig. 4

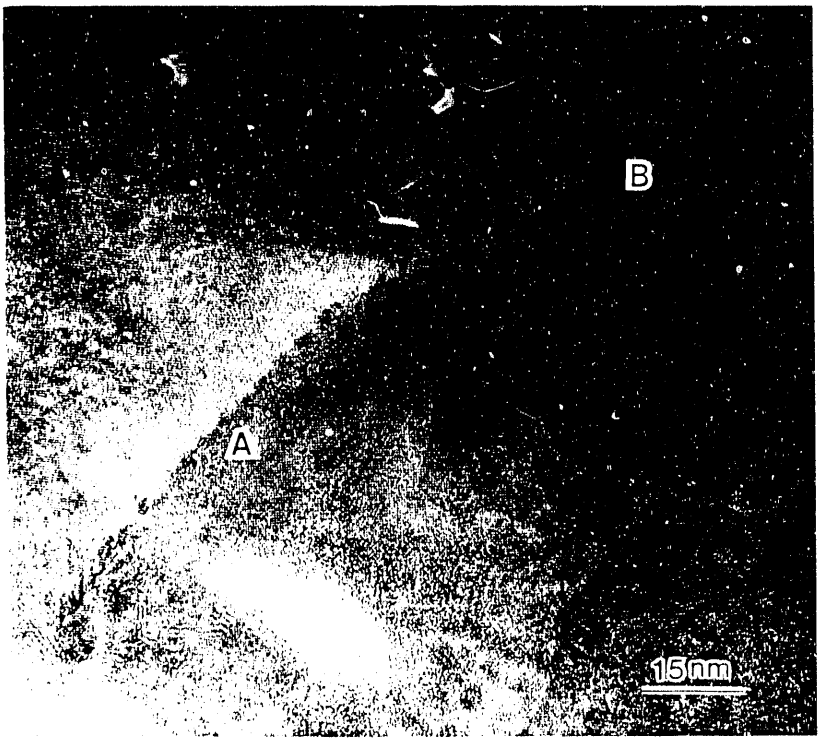

Fig. 5a

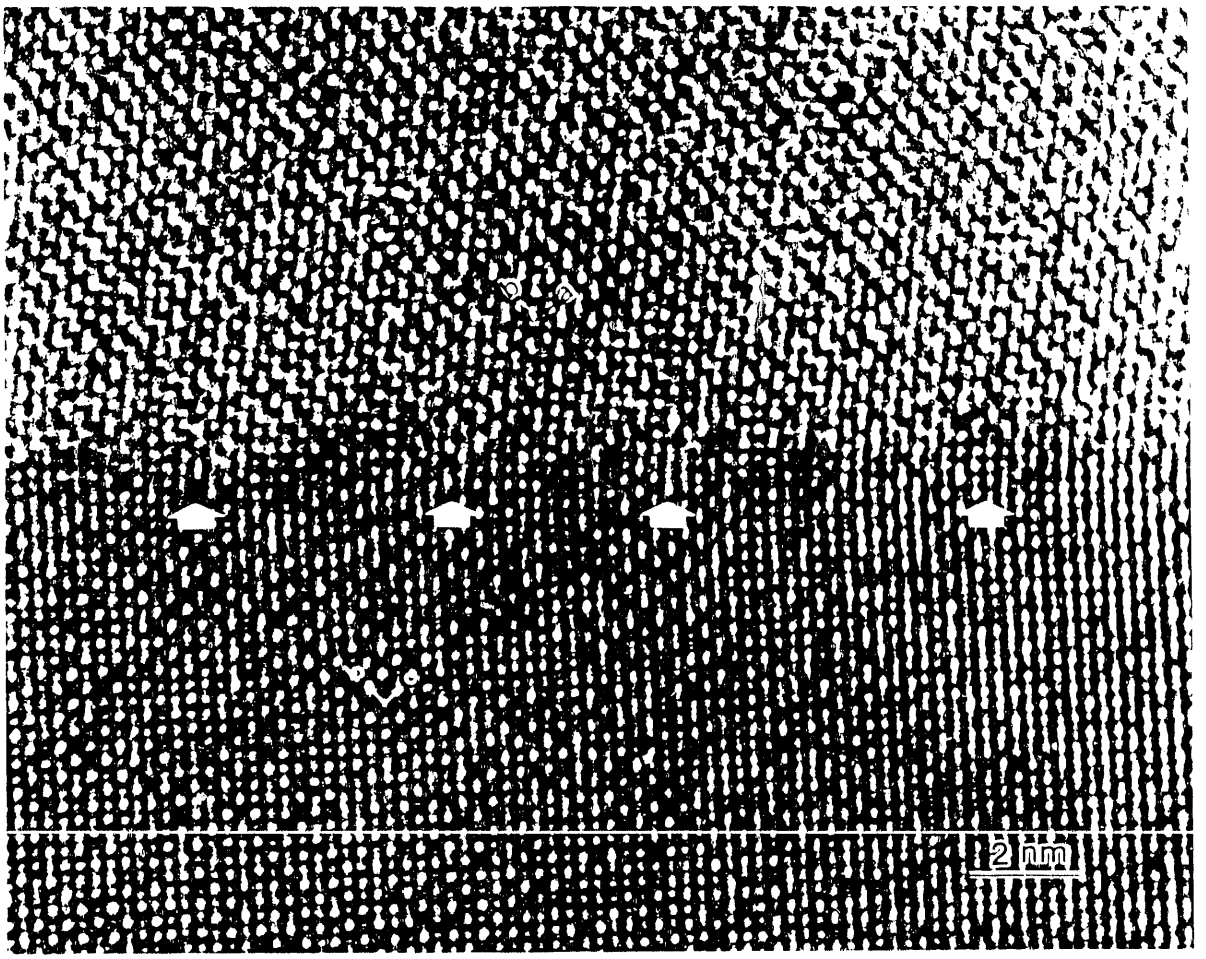

Fig. 5b

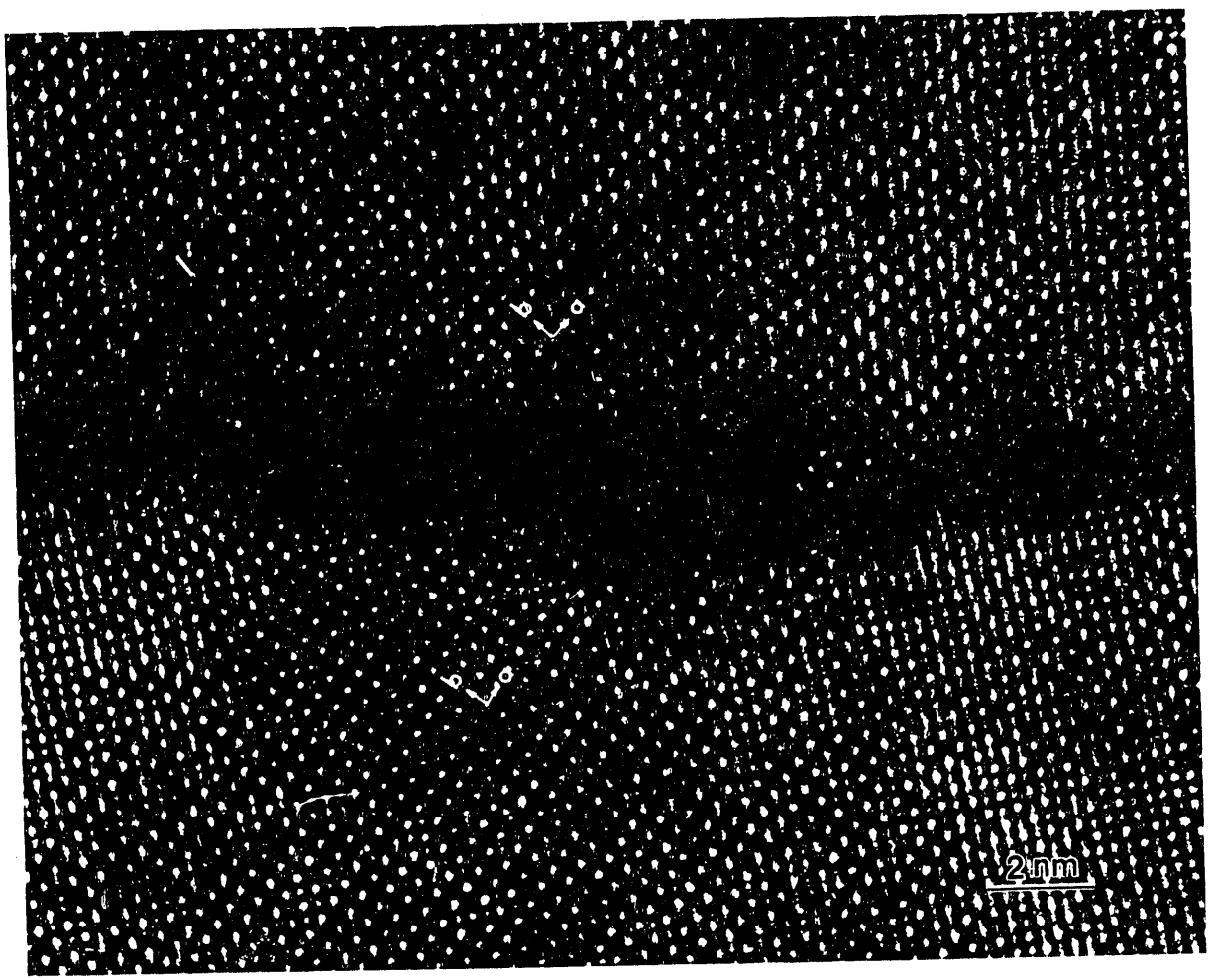

Fig. 5C

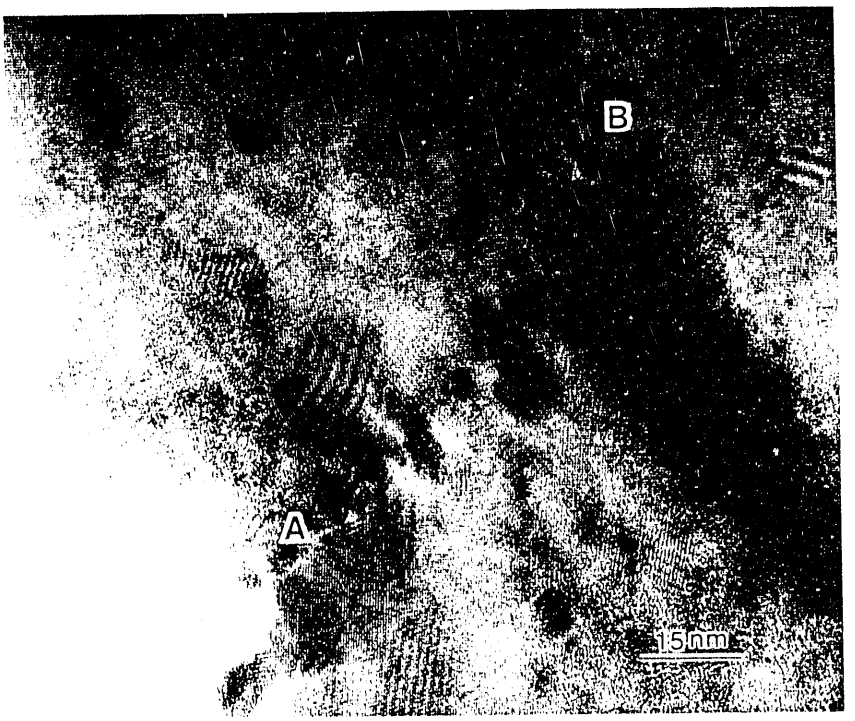

Fig. 6a

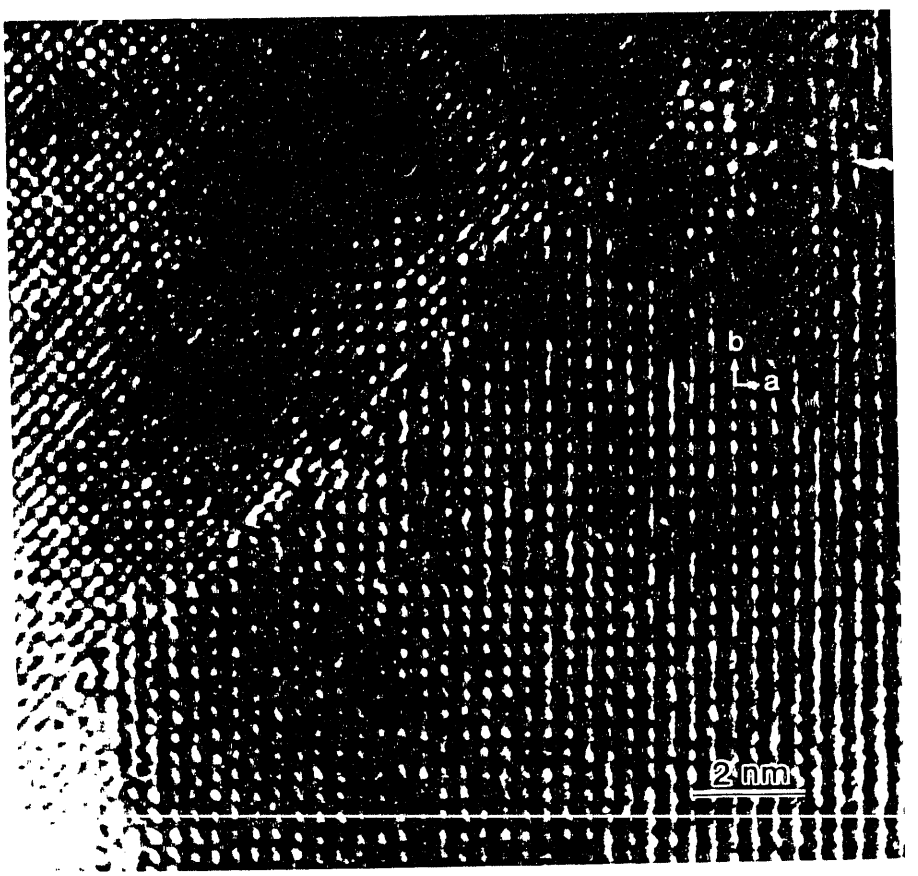

Fig. 6b

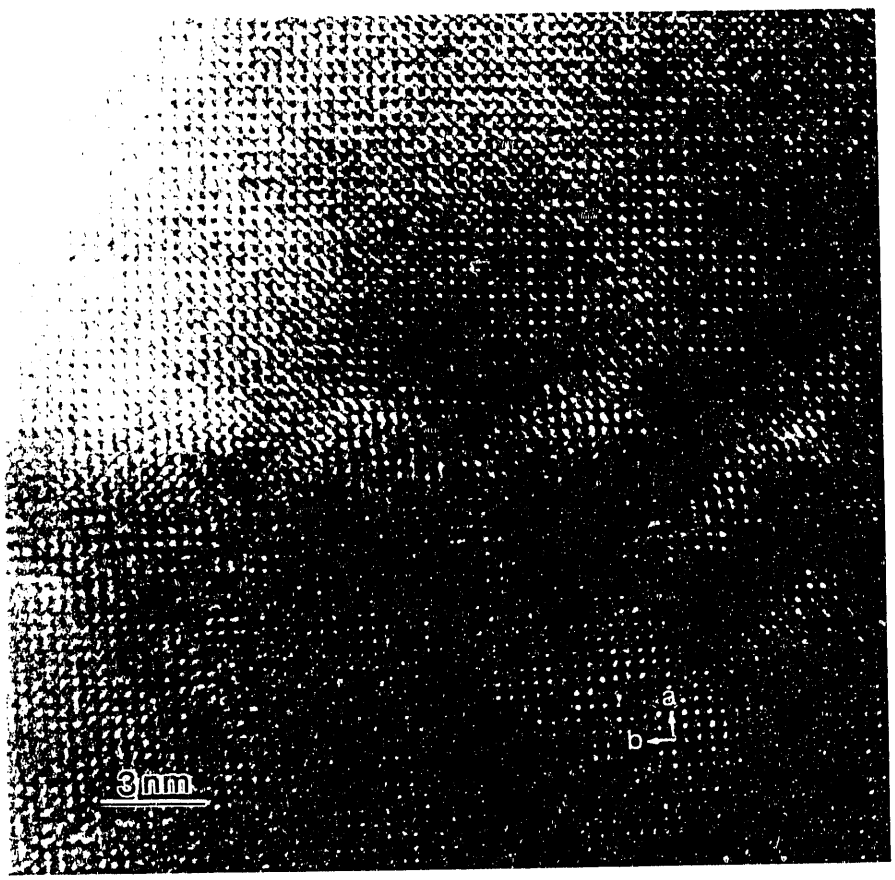

Fig. 6C

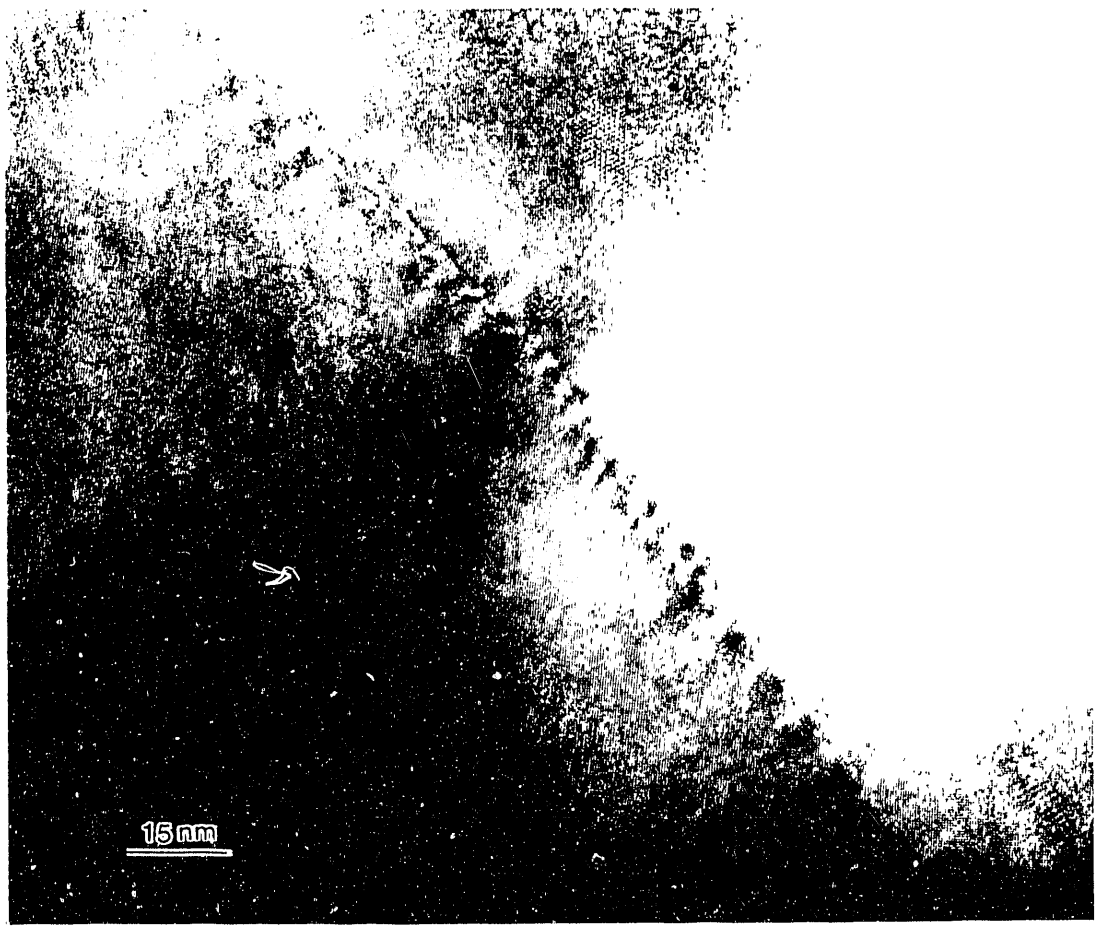

Fig. 7a

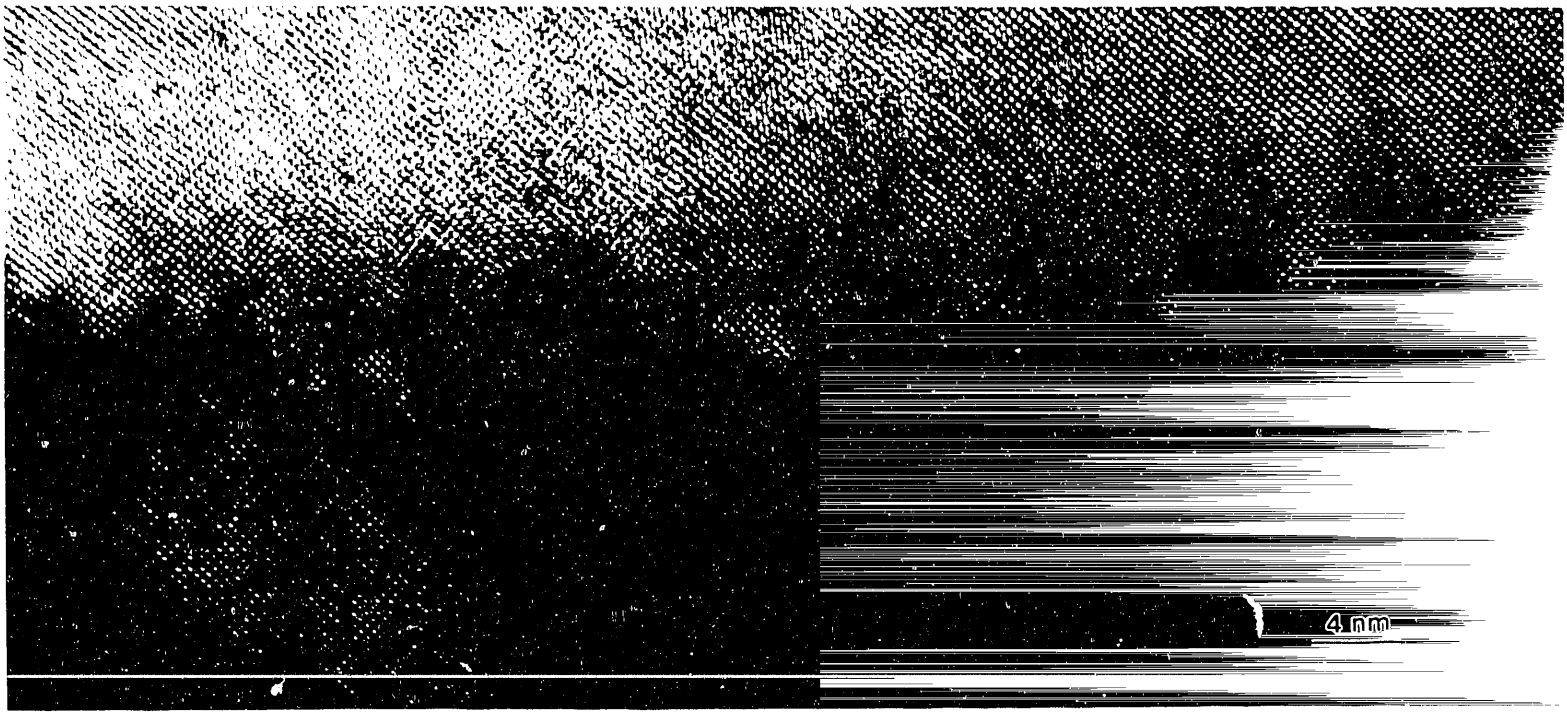

Fig. 7b

Fig. 8

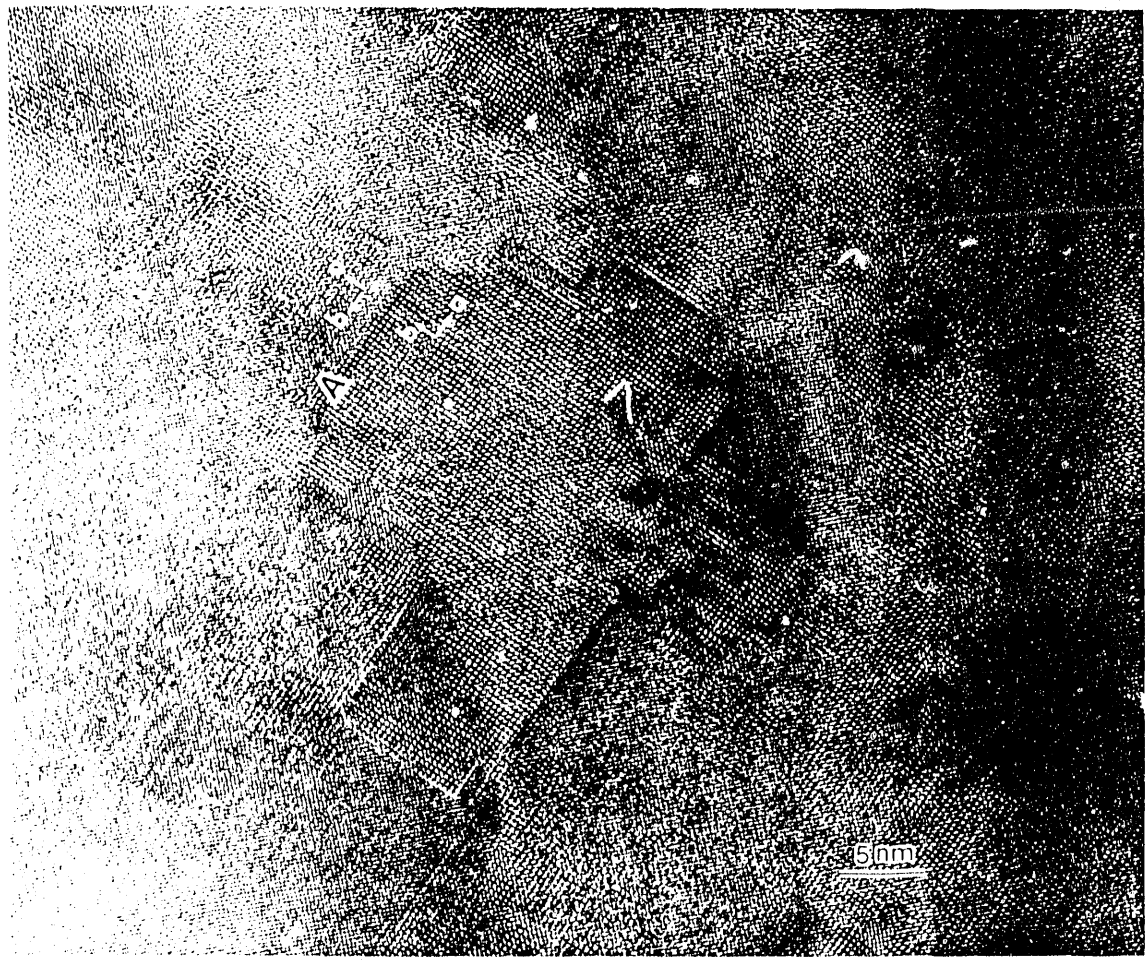

Fig. 9a

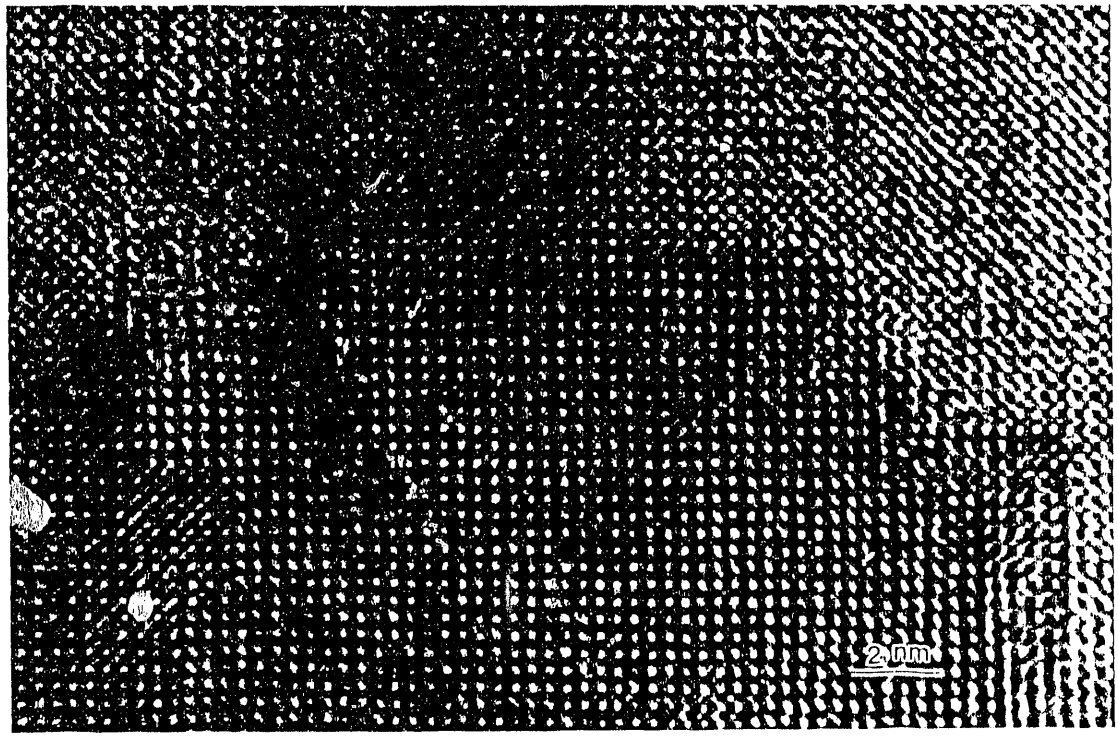

Fig. 9b

-END-

DATE FILMED

01 / 29 / 91